Table 3. Characteristics of radio bursts estimated using 1st harmonics of type-II and their associated solar events and geomagnetic storms.

	Burst Event				X-ray Flare				CME		Shock Characteristics					Dst (nT)
	Date (UT)	Fs (MHz)	Drift rate (MHz/s)	Height (Rs)	Start (UT)	Class	NOAA	Location	Onset (UT)	Speed (km/s)	X	M	Vs (km/s)	VA (km/s)	B (G)	
1	[illegible]/2024	68	-0.077	1.50	21:05	M1.5	-	S18W46	21:24	496	1.7778	1.64	383	233	0.53	-56
2	23/04/2024 17:46	40	-0.047	1.83	17:55	M2.9	13638	S17W58	18:00	321	1.6531	1.53	296	194	0.35	-50
3	03/05/2024 18:52	58	-0.243	1.61	18:40	C7.5	13638	N26W03	18:52	-	21717	2.06	1480	717	1.39	-72
4	03/05/2024 20:30	50	-0.042	1.69	20:12	C4.0	-	N09E33	19:53	429	1.6979	1.57	322	205	0.34	-72*
5	09/05/2024 17:32	87	-0.133	1.41	17:23	X1.1	-	S17W28	17:23	595	1.6305	1.51	490	324	1.07	-412**
6	14/05/2024 12:45	50	-0.058	1.65	112:40	X1.2	13668	S17W89	12:53	605	1.4400	1.34	322	325	0.66	-102
7	14/05/2024 16:51	49	-0.104	1.69	16:46	X8.7	13664	S18W89	16:53	878	1.4792	1.37	490	604	1.14	-86
8	14/05/2024 17:08	50	-0.154	1.68	17:25	M4.5	-	N17W59	17:23	773	1.3061	1.23	437	947	2.02	-114
9	29/05/2024 14:49	40	-0.096	1.80	14:11	X1.4	-	S20E66	14:53	735	1.4400	1.34	832	726	1.07	-56
10	21/06/2024 23:52	39	-0.043	1.82	23:58	C7.4	-	N13W59	23:14 8	552	1.4854	1.38	1171	335	0.47	-28
11	04/07/2024 14:49	49	-0.047	1.68	14:06	M1.0	13723	S21W74	14:42	261	1.8906	1.75	978	208	0.35	-30
12	25/07/2024 15:39	50	-0.092	1.75	15:27	M1.3	13751	S07W85	14:53	271	1.6044	1.48	463	502	0.76	-74
13	01/10/2024 22:23	85	-0.132	1.40	21:58	X7.1	13844	S15W03	23:12	331	1.8595	1.72	365	292	0.81	-32
14	03/10/2024 12:32	85	-0.141	1.40	12:08	X9.0	13842	S15W05	11:36	177	1.9600	1.82	747	294	0.75	-158
15	03/10/2024 20:16	85	-0.226	1.43	20:09	M6.7	-	S07W45	20:36	597	1.3314	1.25	503	747	2.47	-158*
16	07/10/2024 20:05	85	-0.159	1.50	19:02	X2.2	-	S16W62	19:53	2124	1.3540	1.27	537	614	1.72	–314

*Geomagnetic storm due to interacting CME events.

**Largest geomagnetic storm of solar cycle 25 (to this date).

Author Manuscript

This is the author manuscript accepted for publication and has undergone full peer review but has not been through the copyediting, typesetting, pagination and proofreading process, which may lead to differences between this version and the Version of Record. Please cite this article as doi: 10.1029/2024EA004114.

This article is protected by copyright. All rights reserved.

Author Manuscript

SunRISE Ground Radio Lab: Monitoring Solar Radio Bursts with an Expansive Array of Antennae at High Schools Nationwide

Akhavan-Tafti, M. [1]; Soni, S. L. [1]; Higgins, C. [2]; Fung, S. [3]; Lepri, S. [1]; Lux, J. [4]; Lazio, J. [4]; Romero-Wolf, A. [4]

[1] Climate and Space Sciences and Engineering, University of Michigan, Ann Arbor, MI
[2] Middle Tennessee State University, Murfreesboro, TN
[3] NASA Goddard Space Flight Center, Greenbelt, MD
[4] Jet Propulsion Laboratory, California Institute of Technology, Pasadena, CA

Key Points

1. SunRISE Ground Radio Lab promotes STEAM at high schools nationwide through hands-on activities focused on space sciences and engineering.
2. Ground-based antennae are deployed at 18 high schools nationwide, engaging up to 2,500 students in collecting & cataloging solar radio bursts.
3. Type II solar radio burst observations are used to characterize the corresponding coronal mass ejections and solar source.

A. Abstract

The Sun Radio Interferometer Space Experiment (SunRISE) Ground Radio Lab (GRL) is a Science, Technology, Engineering, Arts, and Mathematics (STEAM) project, sponsored by NASA's SunRISE mission and organized by the University of Michigan College of Engineering. The project aims to engage and train the next generations of scholars. To achieve this, the project deployed antennas to 18 high schools nationwide to observe solar radio bursts (SRB). SRBs are defined as low-frequency radio emissions emanated by accelerated electrons associated with extreme solar activity, including solar flares and coronal mass ejections (CMEs). Type II SRBs were found to predominantly correspond to coronal shocks caused by CMEs, highlighting particle acceleration events in the solar atmosphere and interplanetary space. These bursts can act as early warning signs of upcoming solar disturbances which can lead to geomagnetic storms. The type II bursts were then investigated to estimate the corresponding shock and Alfvén speeds: $277<v_{shock}<1480$ km/s and $194<v_A<947$ km/s at heliocentric distances of around 1–2 solar radii, respectively. The Alfvén Mach number was further found to be $1.2<M_A<2$, while the measured magnetic field strength followed a single power law of $B(r) = 0.3\ r^{-2}$, where *r* represents the heliocentric distance. Our results were found to agree with previous studies. Through SunRISE GRL, an ever-expanding catalog of SRBs is being collected by high school students nationwide, curated by a team of solar physics experts, and made publicly available to the scientific community to make progress toward the SunRISE mission's objectives.

This article is protected by copyright. All rights reserved.

Author Manuscript

B. Introduction

Solar radio bursts (SRBs) are low-frequency radio emissions emanated by accelerated electrons associated with extreme solar activity, including solar flares and coronal mass ejections (CMEs) (Cane et al., 1986; White et al., 2011; Alibay et al., 2017). Within the metric wavelengths, SRBs are categorized into different types, ranging from type I to type V (Hettiarachchi et al., 2024). The categorization is based on the radio burst's appearance on the dynamic spectrum, which illustrates the temporal fluctuations in spectral intensities. Types of radio bursts are commonly associated with different phenomena of solar activity. For example, type-II radio bursts are associated with CMEs (Smerd et al.,1975, Gopalswamy et al., 2005, Knock & Cairns ., 2005). Drift in their frequency over time, or drift rate, coincided with the transmission of shock associated with CMEs, as they moved from regions of higher to lower density media (Soni et al., 2021). The type-III radio burst represents a sharp increase in intensity across a wide frequency range, marked by a sudden brightening in dynamic spectra, as depicted in Figure 1. Type-III radio bursts are closely tied to the abrupt release of energetic electron beams during solar flares or magnetic reconnection events (Suzuki and Dulk, 1985; Reid and Ratcliffe, 2014; Reid et al., 2020). Table 1 contains a description of the types of radio bursts, their appearance in dynamic spectra, as shown in Figure 1, and possible source, based on the current understanding of the emission mechanisms.

The underlying mechanisms responsible for the generation and propagation of SRBs can be determined by using open-source data and employing simple observational techniques and data analysis methods. Previous studies have revealed that intense radio bursts often precede CMEs, serving as early indicators of these extreme solar events.

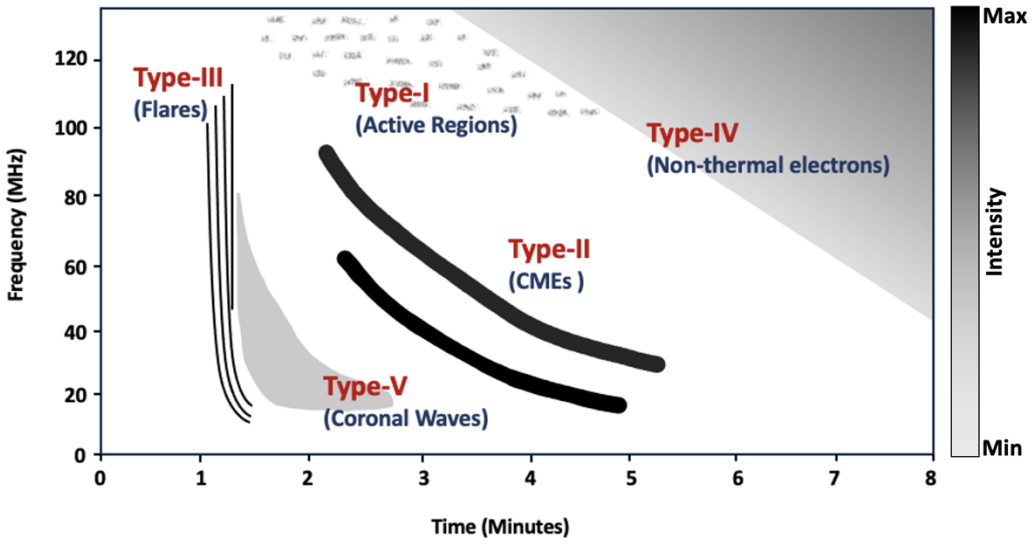


Figure 1: Categorization of SRBs based on their appearance within a dynamic spectrum. Type II solar radio bursts are characterized by their unique two-banded emission, consisting of the fundamental frequency and its harmonic, both of which exhibit a gradual drift toward lower frequencies.

This article is protected by copyright. All rights reserved.

CMEs linked to strong radio bursts tend to exhibit higher speeds and stronger magnetic fields, making them more likely to cause severe geomagnetic storms upon interacting with the Earth's magnetosphere (Kumari et al., 2023). This interaction results in a more intense geomagnetic response. To that end, monitoring SRBs from different frequency channels offers the opportunity to enhance our geomagnetic storm prediction capabilities, and therefore, improve our preparedness and mitigation strategies for space weather-related disruptions.

Table 1: Description of SRB types, their appearance in dynamic spectra and their associated possible origins. For more information, refer to Benz (2009; 2009).

SRB Types	**Appearance in Dynamic spectra**	**Source**
Type-I	Background continuum	Sunspots and active regions on the Sun's surface
Type-II	Narrow-band drifting structures (seconds to minutes)	CMEs: energetic electrons accelerated around coronal shocks
Type-III	fast-drifting features (few seconds)	Flares: fast, energetic electrons releasing from the reconnection site and escaping outward (or inwards) along field lines.
Type-IV	Wideband continuum in higher frequencies	Acceleration of nonthermal electrons to high energies
Type-V	Wider spectral regime near Type-III	Strongly scattered energetic electrons by coronal waves.

Type II solar radio bursts are generated by a propagating shock associated with CMEs. When a shock wave passes through plasma, it can accelerate charged particles, especially electrons, to high velocities. These accelerated electrons form what is known as plasma beams or electron beams. These beams are highly energetic and travel along the magnetic field lines in the plasma, moving at speeds close to the speed of light. As the high-energy electron beams travel through the ambient plasma, they induce disturbances in the local electron density. These disturbances result in the generation of Langmuir waves, which are a type of electrostatic plasma wave characterized by oscillations of electrons around their equilibrium positions. Langmuir waves are unstable; they can interact with other plasma waves or particles, leading to the emission of electromagnetic radiation, particularly at radio frequencies. The signature of this shock propagation can be identified as drift in SRB signature in dynamic spectrum. The frequency drift towards the lower frequencies indicates that the density of electrons is falling. This variation generally shows that in the solar atmosphere, the burst drivers move higher in height where plasma density is generally lower. In other words, shock/CME

This article is protected by copyright. All rights reserved.

Author Manuscript

propagates away from the Sun. The emitted plasma frequency f_p is related to the electron density n_e by the relation given by $f_P = 9{,}000\ \sqrt{n_e}$ (for the fundamental band; Soni & Ebenezer ., 2022; also, see review by Melrosa (2017)). In that scenario, type II radio bursts are an important tool to determine the shock/CME kinematics.

Radio waves released from solar flares and CMEs known for their intense and transient radio emissions, have the potential to impact the Earth's ionosphere, leading to perturbations in the ionospheric electron density (Tsurutani et al., 2009). Spaceborne observation of SRBs avoids ionospheric interference and provide a baseline measurement of the bursts' characteristics. Ground-based measurements receive the radio waves after they have passed through the ionosphere. Ionospheric disturbances, such as increased ionization due to solar activity or geomagnetic storms, can affect the propagation of radio waves through the ionosphere. This can lead to signal delays, phase shifts, and amplitude variations in the received radio signals. The disturbances in the received signals can be identified by comparing spaceborne and ground-based observations. The ionospheric conditions can then be inferred from the identified radio signal disturbances. This information is essential for understanding how solar activity impacts Earth's ionosphere and can affect communication and navigation systems.

C. Solar Radio Burst Observations in the SunRISE Era

Spaceborne observations of SRBs have often relied on single-node antenna aboard a spacecraft, such as the WIND mission (Bougeret et al., 1995). This will change by the Sun Radio Interferometer Space Experiment (SunRISE) mission, wherein an array of six small satellites will aim to observe SRBs simultaneously (frequency range 100 kHz - 23 MHz) (Kasper et al., 2020). From the geosynchronous orbit (GEO), the six satellites will create a large (~100 km^2) single-aperture radio telescope, aiming to investigate 1) the generation of solar energetic particles by measuring the location of associated type II radio emissions, and 2) the variable magnetic connection between active regions and the inner heliosphere by reconstructing magnetic field lines associated with Type III radio bursts.

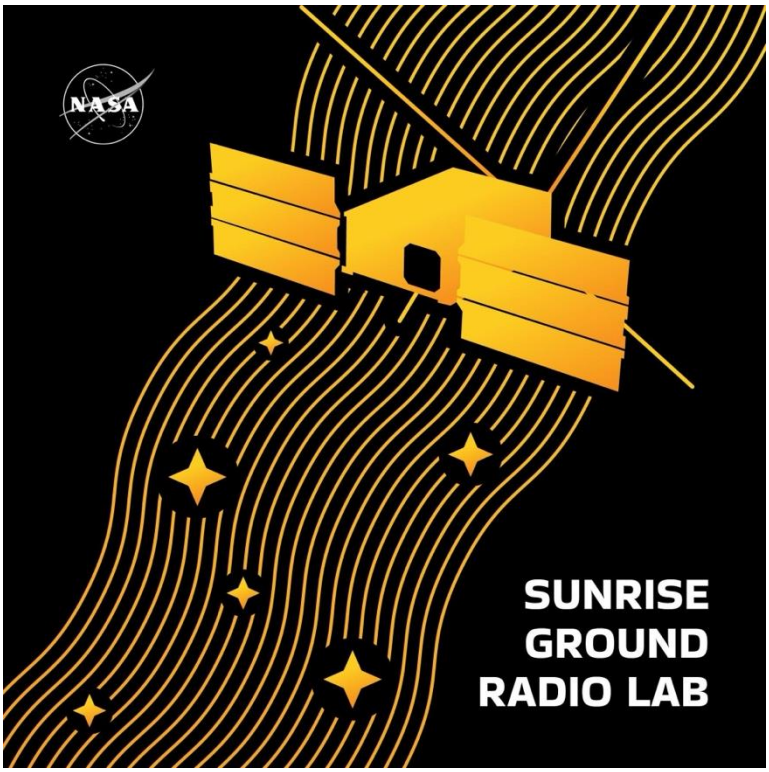


Figure 2: SunRISE GRL is a STEAM program aiming to engage and train the next generations of scholars.

This article is protected by copyright. All rights reserved.

SunRISE Ground Radio Lab (GRL; Figure 2) project is a Science, Technology, Engineering, Arts, and Mathematics (STEAM) program aiming to engage high school students, while bringing together undergraduates, graduates, and postdocs to participate in the training of the next generations of scholars (Akhavan-Tafti, 2024). The SunRISE GRL community utilize two types of ground radio antenna to detect SRBs: dual dipole antenna (DDA) and long wavelength array (LWA). SunRISE GRL recruits and trains high school and undergraduate students nationwide to contribute to antenna design, fabrication, and installation, as well as data collection, categorization, and analysis.

i. Instrumentation

1. Dual dipole antenna

The dual dipole antenna (DDA) is coupled with a radio receiver and software (Radio-Sky Spectrograph and SDRPlay2RSS program). DDA is ideal for affordably monitoring emission from the Sun, as well as Jupiter and the galaxy. The radio operates within a range of 16 to 24 MHz. Figure 3 shows the antenna configuration: (a) a dipole antenna mounted atop two modular masts, (b) installed in parallel from a second dipole antenna. The mast and componentry are Polyvinyl Chloride (PVC) pipes. The radio antenna design, fabrication, and assembly instructions can be found here: tinyurl.com/SunRISEGRLPublicDocs.

Since installation across more than a dozen high schools nationwide, SunRISE's DDAs have catalogued hundreds of SRBs. The catalog is curated and made publicly accessible. It is an ongoing effort maintained by students and mentors, providing valuable data to the scientific community in support of the broader objectives of the SunRISE mission. Please refer to Appendix A for more information.

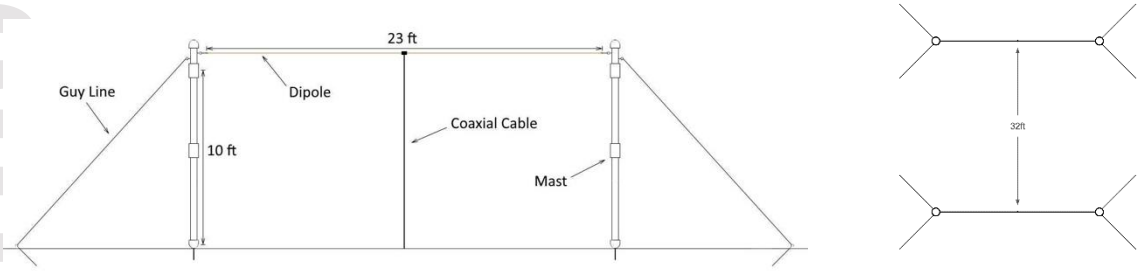


Figure 3. (a) Side-view, and (b) top view schematic of a dual dipole antenna. A dual dipole antenna comprises two sets of dipole antennas. Each dipole antenna is made up of two copper wires connected via a connector that also attaches to an axial cable going to a receiver. The dipole is mounted atop two 10ft-tall modular masts that are anchored 23ft apart. The two dipole sets are installed in parallel at a distance of 32ft.

This article is protected by copyright. All rights reserved.

Author Manuscript

Author Manuscript

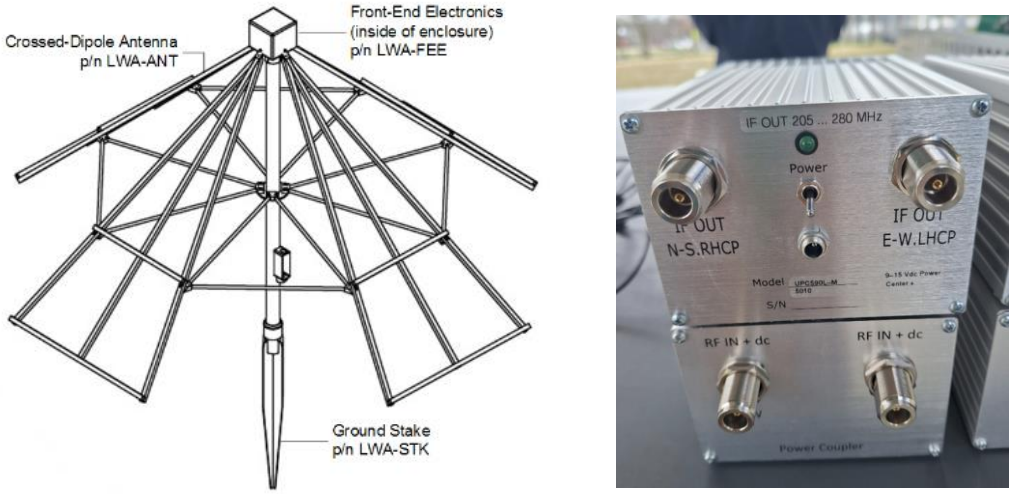


Figure 4. (Left) Diagram of an LWA antenna. Each of the two dipoles consists of two triangular aluminum frame elements sloping down 45° and supported from the steel center post by non-conductive horizontal fiberglass rod braces. Each element is 1.5 m long x 0.8 m wide. At the base of the antenna is a 3 m x 3 m galvanized wire mesh ground screen. The peak (apex) of the two dipoles is 1.5 m above ground level with the dual active balun assembly in the gray enclosure at the top (S. Nelson, 2014). (Right) LWA dual-frequency receiver and dual-channel heterodyne up-converter –commercially referred to as e-Callisto.

2. Long Wavelength Array

The Long Wavelength Array (LWA) is a radio telescope system designed for the observation of SRBs and other astrophysical phenomena at low frequencies. Comprising multiple antenna stations, the LWA operates effectively within the frequency range of 5 to 85 MHz, making it particularly adept at detecting low-frequency radio emissions from solar events, such as solar flares and CMEs (Ellingson et al., 2009; 2010; 2012; Kassim et al., 2007). The LWA's data acquisition system has a 1 Hz sampling rate, which is adequate for capturing the rapid dynamics associated with SRBs (Hick et al., 2018). The integration of multi-frequency observations allows LWA to differentiate between genuine solar signals and interference, thus enhancing the reliability of the collected data (Liu et al., 2020). Visit www.e-callisto.org, for more information.

As shown in Figure 4, the LWA antenna is coupled with a dual-frequency receiver, a dual-channel heterodyne up-converter, a power coupler, and a standard Windows-based computer for data processing and analysis. The other parts of the antenna include the active pre-amplifier at the apex to enhance the system's sensitivity, a support structure, and a ground screen made of steel grid cells of size 3 m × 3 m that prevents back reflection and reduces the susceptibility to changeable soil conditions. The antenna's base length is ~ 0.5 m, and the vertical height is ~ 1.5 m. A detailed overview of the components and geometry of the LWA antenna was presented by Hicks et al., (2012).

This article is protected by copyright. All rights reserved.

Author Manuscript

4. Results and Discussion

a. Case Study 1: Multi-Frequency Observations of a Type II SRB

Figure 5 shows a Type-II radio burst observed at a SunRISE DDA station, located in Skyline High School, Ann Arbor, MI. Panel b shows the corresponding event observed using a SunRISE LWA, located nearby at Peach Mountain Observatory, Dexter, MI. Panel c shows the same event observed by the WAVES instrument aboard the WIND spacecraft. Frequency ranges of the different spaceborne and ground-based radio telescopes are listed in Table 2.

Table 2: List of different ground and space-based radio observatories with their frequency ranges and observable associated location.

Instrument	**DDA**	**LWA**	**Wind/WAVES**	**SunRISE (Kasper et al., 2020)**
Frequency range	16-24 MHz	45-180 MHz	20 kHz-14 MHz	100 kHz to 23 MHz
Solar Height	~1.5-2.5 R_S	~1.2-2 R_S	Interp. medium	1.5 R_S to Interplanetary medium

The coronagraphic image and height-time profile of the associated CME are presented in panels d and e. The LWA antenna covered the frequency range 5-85 MHz (dynamic spectra in blue box), The first signature of radio burst was observed at 17:44 UT on April 23, 2024, corresponding to the 1.2 R_S analyzing height-time profile of CME (blue box in CME height-time profile). The shock formation height can be estimated using Newkirk model (Newkirk, 1961). A type II radio burst signature, shortly following the timing of the LWA SRB, was observed using the DDA antenna (dynamic spectra in red box), though at lower frequencies (16-24 MHz). This signature corresponds to ~2.5 R_S.

This CME event was radio loud, and traveled at 624 km/s. The CME arrived on Earth on April 23rd, 2024, at 01:24 UTC and generated a moderate geomagnetic storm with a storm index Dst reaching -54 nT, as highlighted in Panel f. The shock associated with the CME arrived on April 26 at 01:24 UT, and minimum Dst was observed at 08:48 UT. The blue, red and green lines in the plot correspond with the detection of SRBs by SunRISE LWA, DDA, and the WAVES instrument aboard the Wind spacecraft, respectively. This example further highlights how our students can contribute to the scientific community by corroborating observations using a different frequency band than existing space weather assets. This example also shows how our students can use other existing assets to verify whether their observed SRB and analyses agree with state-of-the-art observations.

b. Case Study 2: Using Type II SRB Observations to Characterize the Corresponding CME and Solar Source

Type-II bursts are produced by shocks in the corona and the interplanetary medium. Band splitting in Type-II radio bursts (both in fundamental and harmonic band) are due to the plasma emission from upstream and downstream shock regions (Smerd et al., 1974;

This article is protected by copyright. All rights reserved.

Vršnak et al., 2001; Vasanth et al., 2014; Soni et al., 2021). These emissions can be seen in radio spectrographs as split bands (upper and lower) both in fundamental (F_U and F_L) and harmonic frequencies (H_U and H_L) close to a ratio of 1:2. Figure 6 shows an example of band splitting of type II radio bursts associated with the CME event discussed in Figure 5. On April 23, 2024, a CME followed a flare class M2.9 from NOAA active region 13638, located at N26W58 on visible solar disk.

i. CME characteristics

The characteristics of the CMEs can be derived from the Type II SRBs with the aid of a series of mathematical tools including the Gopalswamy model (Gopalswamy et al., 2011)

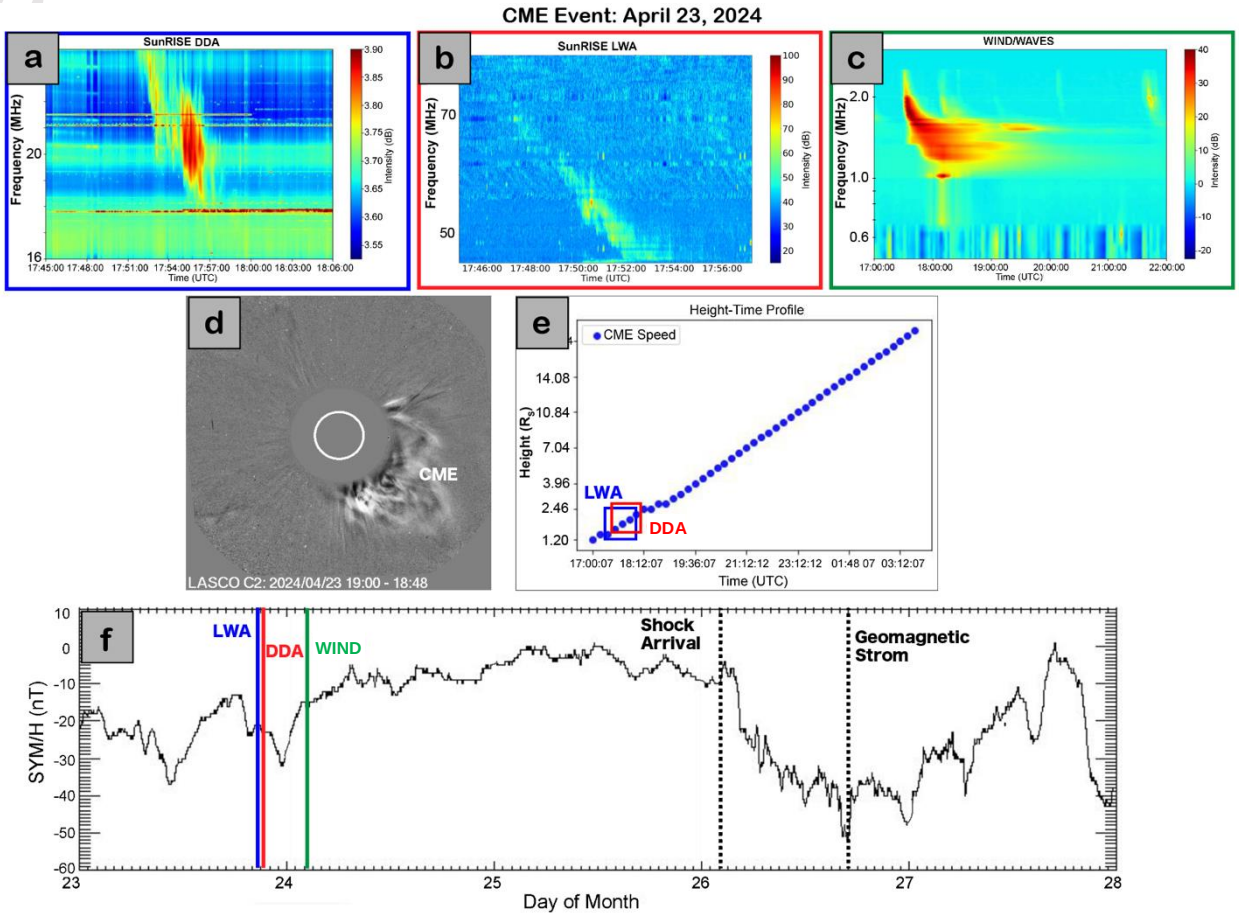


Figure 5: (a) Dynamic spectra observed by DDA, (b) Dynamic spectra observed by LWA, (c) Dynamic spectra observed by WIND/WAVES, (d) snapshot of Associated CME from LASCO/SOHO C2 coronagraph, (e) height-time profile of CME, and (f) geomagnetic response (storm index Dst) associated with the CME event and type II radio burst.

This article is protected by copyright. All rights reserved.

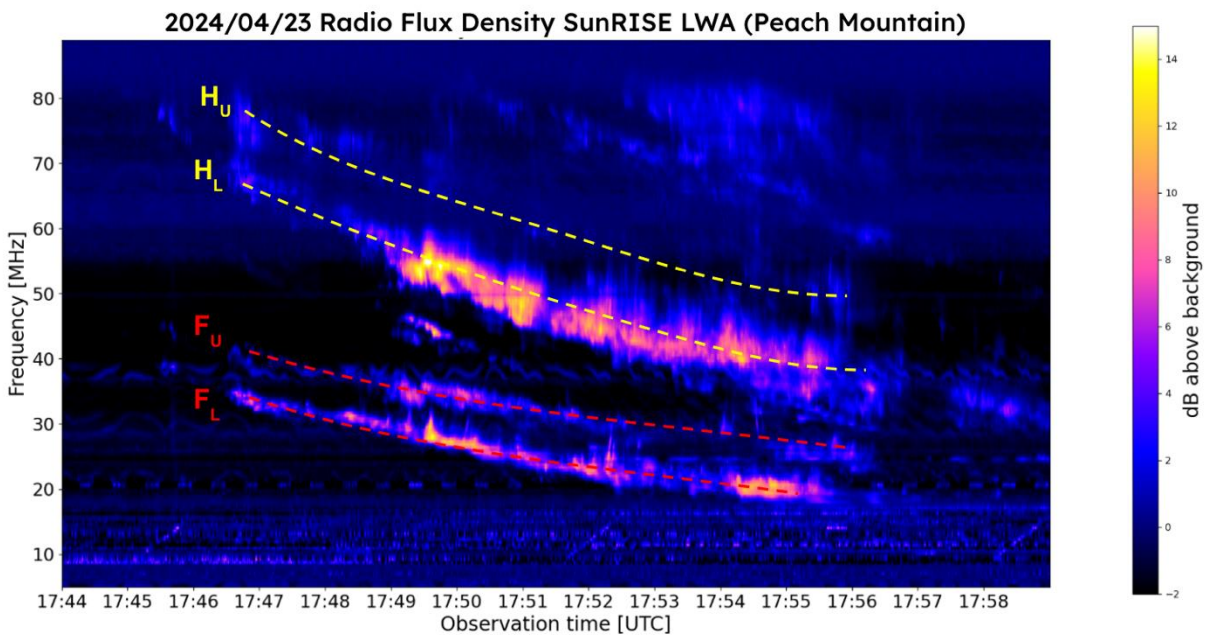


Figure 6: Dynamic radio spectra observed by SunRISE LWA antenna, located at Peach Mountain Observatory, Dexter, MI, USA. The spectrum shows a type II radio burst associated with the CME event occurring on April 23, 2024. The red dotted lines over bright signatures show fundamental bands (F_U and F_L) of type–II radio bursts and yellow shaded lines show the harmonic bands (H_U and H_L) of type II radio bursts.

and the Newkirk model (Newkrik., 1967).

First signature (frequency and time) of type II radio burst on dynamic spectra is associated with the shock formation location over the solar atmosphere. At the fundamental mode, the plasma frequency fp (Hz) is related to the electron density n_e (cm^{-3}) by the relation given by $f_p = 9000\sqrt{n_e}$, or

$$n_e = \left(\frac{f}{k \times 8.977 \times 10^{-3}}\right)^2,$$

where f is the frequency at a certain point in the type II SRB, and k is the harmonic number, with value 1 for the fundamental band, 2 for the 1st harmonic band, etc. and

$$r = \frac{4.32}{log_{10}(\frac{n_e}{newkirk \times 4.2 \times 10^4})},$$

where $newkirk$ is a coefficient in the Newkirk model to approximate an active corona to a quiet corona, chosen as 1.8 (Newkirk et al., 1967).

This article is protected by copyright. All rights reserved.

Author Manuscript

The frequency drift towards the lower frequencies indicates that the density of electrons is falling. This variation generally shows that in the solar atmosphere the burst drivers move towards the larger heights and lower densities. For this reason, Type-II radio bursts are an important tool to determine the CME shock speed. Gopalswamy et al. (2011) estimates the characteristics of CME shocks with type II radio burst fundamental band observations. It suggests that the shock speed (V_s) can be calculated using:

$$\mathrm{V_s} = -\frac{2r}{\alpha}\left(\frac{1}{f_0}\right)\left(\frac{df}{dt}\right),$$

where r is the height in solar radius at which the shock was generated, f_0 is the starting frequency of the fundamental upper band, and $\frac{df}{dt}$ is the average drift rate across the entire fundamental band. α is a fitted value, and since all the type II SRBs observed were generated in the range of 1~2 solar radius, α can be chosen as 6 (Gopalswamy et al., 2011).

Figure 7 shows the modeled CME characteristics, based on the observed Type II radio bursts and their propagation through the solar atmosphere into interplanetary space. In panel a, the relationship between plasma frequency (in MHz) and time is shown,

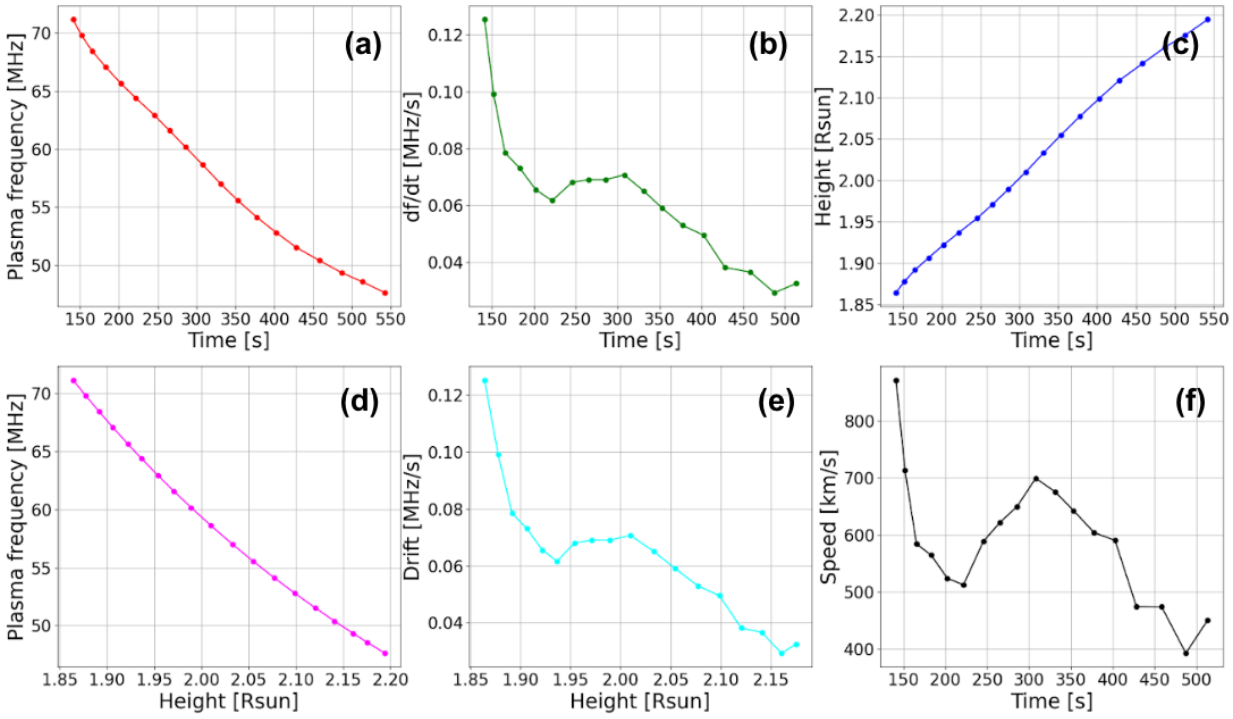


Figure 7. (a) the observed plasma frequency (MHz) and time. (b) rate of frequency change df/dt as a function of time, (c) modeled height-time profile of the Type–II radio burst, (d) plasma frequency profile as a function of height from the solar surface, (e) drift rate changing with distance, and (f) the speed of the shock (km/sec) over time.

This article is protected by copyright. All rights reserved.

Author Manuscript

indicating how plasma frequency decreases over time. Panel b depicts the variation in the rate of change of frequency (df/dt) with time, suggesting how the drift rate evolves. The height-time profile in panel c illustrates the progression of the Type II radio burst into interplanetary space, and panel d highlights the change in plasma frequency as a function of height, revealing the decrease in frequency with increasing distance from the solar surface. Panel e demonstrates how the drift rate varies with distance, providing insights into how radio emissions change as the shock propagates through the corona. Finally, panel f shows the speed of the shock over time.

ii. Modeling the Coronal Ambient Magnetic Field

The Sun's magnetic field significantly influences all coronal heights. In particular, the region between 1 R_S and 3 R_S is crucial model as it serves as the transitional zone between the Sun's photospheric magnetic field and the solar wind. Variations in the magnetic field's structure and its temporal changes impact solar wind conditions and space weather. The band splitting of Type II radio bursts offers a way to estimate the coronal ambient magnetic field along the path of shock waves (Smerd et al., 1975). In our analysis, we estimated the coronal ambient magnetic field strength using the method outlined by Vršnak et al. (2001). This technique utilizes the upstream region's Alfvén speed and density, derived from the fundamental frequencies, to calculate the ambient magnetic field. The density jump χ across the shock wave of the CME can be calculated using:

$$\chi = (\frac{BW}{f_l} + 1)^2,$$

where BW is the approximated bandwidth of the type II SRB, f_l is the lower frequency bound of the type II SRB at the median time point. The Alfvén Mach number (M_A) can be calculated using $M_A = \sqrt{\frac{\chi(\chi+5)}{2(4-\chi)}}$, and $V_A = V_s/M_A$, where V_s denotes the shock speed. The ambient magnetic field strength *B* of the plasma in the proximity of the CME can be estimated using the Alfvén Mach number $B\ (Gauss) = 5.1 \times 10^{-5} \times f_1 \times V_A$.

c. Statistical Analysis: Timing Variability of CMEs and Type II Radio Bursts

A catalog of the modeled characteristics of 16 CME shocks associated with the observed type II SRBs using the LWA antenna are summarized in Table 3. The left-most section lists the type II SRB occurrence date and time, starting frequency, drift rate and corresponding heliospheric location followed by starting frequency, which also corresponds to shock formation height. The second and third sections present the associated flare and CME information along with the source location. Section 2 also includes ancillary information including the coinciding X-ray flares observed by NOAA's

This article is protected by copyright. All rights reserved.

Author Manuscript

GOES satellite, CME eruptions observed in white light by the LASCO/SOHO spacecraft, and the location of solar eruption. Section 4 shows the estimated shock speed and coronal ambient magnetic field strength.

Table 3. Characteristics of radio bursts estimated using 1st harmonics of type-II and their associated solar events and geomagnetic storms.

Type II burst event					Soft X-ray flare				CME		Shock characteristics					Dst
No.	Date (UT)	f_0 (MHz)	Drift rate (MHz s^{-1})	Height $R_\odot$	Start (UT)	Class	NOAA	Location	Onset (UT)	Speed (km s^{-1})	χ	M	V_s (km s^{-1})	V_A (km s^{-1})	B field G	nT
1	22/04/2024 21:19	68	-0.077	1.50	21:05	M1.5	...	S18W46	21:24	496	1.7778	1.6465	383	233	0.534	-56
2	23/04/2024 17:46	40	-0.047	1.83	17:35	M2.9	13638	S17W58	18:00	321	1.6531	1.5307	296	194	0.350	-50
3	03/05/2024 18:52	58	-0.243	1.61	18:40	C7.5	13663	N26W03	18:52	...	2.1717	2.0639	1480	717	1.390	-72
4	03/05/2024 20:20	50	-0.042	1.69	20:12	C4.0	...	N09E33	19:53	429	1.6979	1.5716	322	205	0.345	-72*
5	09/05/2024 17:32	87	-0.133	1.41	17:23	X1.1	...	S17W28	17:23	595	1.6305	1.5104	490	324	1.075	-412**
6	14/05/2024 12:45	50	-0.058	1.65	12:40	X1.2	13668	S17W89	12:53	605	1.4400	1.3458	437	325	0.663	-102
7	14/05/2024 16:51	49	-0.104	1.69	16:46	X8.7	13664	S18W89	16:53	878	1.4792	1.3787	832	604	1.140	-86
8	14/05/2024 17:08	50	-0.154	1.68	17:25	M4.5	...	N17E72	17.23	773	1.3061	1.2364	1171	947	2.029	-114
9	29/05/2024 14:49	40	-0.096	1.80	14:11	X1.4	...	S20E66	14:53	735	1.4400	1.3458	978	726	1.075	-56
10	21/06/2024 23:52	39	-0.043	1.82	23:58	C7.4	...	N13W59	23:48	552	1.4854	1.3840	463	335	0.478	-28
11	04/07/2024 14:35	49	-0.047	1.68	14:06	M1.0	13723	S21W74	14:42	261	1.8906	1.7570	365	208	0.350	-30
12	25/07/2024 15:39	50	-0.092	1.75	15:27	M1.3	13751	S07W85	14:53	271	1.6044	1.4872	747	502	0.768	-74
13	01/10/2024 22:15	85	-0.132	1.40	21:58	X7.1	13844	S15W05	23:12	331	1.8595	1.7261	503	292	0.818	32
14	03/10/2024 12:22	85	-0.141	1.40	12:08	X9.0	13842	S15W03	11:36	177	1.9600	1.8285	537	294	0.750	-158
15	03/10/2024 20:16	85	-0.226	1.43	20:09	M6.7	...	S07W45	20:36	597	1.3314	1.2567	939	747	2.476	-158*
16	07/10/2024 20:05	85	-0.159	1.80	19:02	X2.2	...	S16W62	19:53	2124	1.3540	1.2751	783	614	1.722	-341

*Geomagnetic storm due to interacting CME events.
**Largest geomagnetic storm of solar cycle 25 (to this date).

Some of the calculated shock speed V_s is larger than the white-light speed, such as on May 29, 2024. One plausible explanation is that the white-light results are only the 2D projection of the true 3D speed V_s. In contrast, on May 14, 2024, at 12:45UT, the white-light speed exceeds that of Vs, thus suggesting that the source location of type II SRB was the flanks of the CMEs, which inherently travels at lower speeds than the CME nose (Soni & Ebenezer ., 2022).

In general, the observed start times of type II SRBs do not follow a strict temporal pattern relative to CME eruptions. In some cases, type II bursts are detected before the onset of the associated CME, indicating that the shock wave may form early in the event, possibly as a result of preceding flare activity. Conversely, there are instances where type II bursts begin after the CME has fully erupted, suggesting that the shock wave forms at a later stage as the CME accelerates through the corona. The difference in CME onset and the observation of type II SRBs is presented in Figure 8. This variability highlights the complex interaction between the CME dynamics, shock formation, and radio emission processes in the solar atmosphere.

Author Manuscript

This article is protected by copyright. All rights reserved.

Author Manuscript

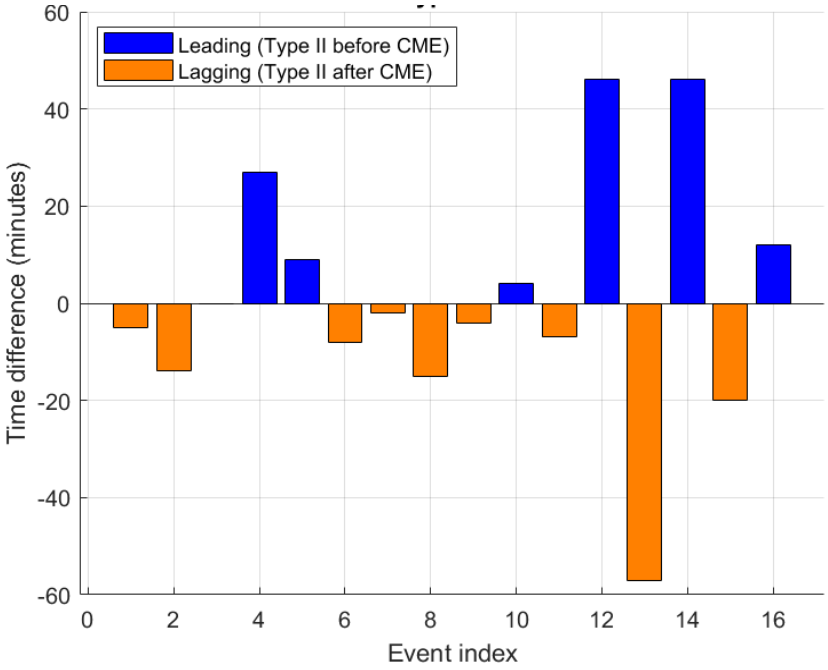


Figure 8. The time differences between the CMEs onset time and the start time of the type II SRBs

5. Conclusions

In this study, we summarize preliminary analyses of the SunRISE GRL observations, using dual dipole antenna and long wavelength array antenna deployed at high schools nationwide. Our analysis indicates:

- Type II radio bursts are found to coincide with weak to extreme geomagnetic storms. In particular, Type-II bursts corresponding to the same Earth-bound halo CME were detected by multiple observatories at least 48 hours earlier than reported by in-situ and ground-based space weather assets solely monitoring for changes in near-Earth magnetic and plasma properties. This means that the SunRISE mission and GRL observations can potentially serve as crucial indicators of impending geomagnetic disturbances caused by CMEs.
- Key type II SRB parameters, including bandwidth, drift rates, and starting frequency, are utilized to derive associated shock characteristics such as shock speed, Alfvén speed, Mach number, and magnetic field strength.
    - The estimated shock and Alfvén speeds fall between 277–1480 km/s and 194– 947 km/s, respectively, at a heliocentric distance of approximately 1–2 solar radii (Rs). These findings align with previous research, where shock speed (e.g., Cunha-Silva et al., 2015; Minta et al. 2023), was identified to range between 200 and 810 km/s. Similarly, Alfvén speed was found at different solar heights to range between 550–400 km/s (solar heights

This article is protected by copyright. All rights reserved.

between 1.6–2.1 R_S; Cho et al., 2007), 140—460 km/s (solar heights between 1.2–1.5 R_S; Gopalswamy, 2011), and 259–982 km/s (solar heights between 3–15 Rs; Kim et al., 2012).

- The Mach numbers derived in this study $1.2 \leq M_A \leq 2$ within the same heliocentric distance, align with the findings of Mann et al. (2022) and Su et al. (2022), while the magnetic field strength (in units of Gauss, G) estimates $B(r) = 0.3\ r^{-2}$, are in agreement with those reported by Vršnak et al. (2002) and Ramesh et al. (2010), who observed field strengths between 1–8 G at 1.6 R_S and 6–5 G at 1.5–1.7 R_S, respectively.
- 15 of the 16 LWA Type II SRB events are associated with moderate to super-intense geomagnetic storms. The event observed on May 09, 2024 was associated with the most intense geomagnetic storm observed in solar cycle 25 so far and also in the last two decades with the Dst value -412 nT.

- The initiation of a Type II radio burst can precede or follow the onset of associated CMEs. This timing discrepancy arises from the interaction of CME-driven shocks with the coronal environment, where factors like CME velocity, coronal density, and shock formation dynamics influence the generation of these distinctive radio emissions.

6. Acknowledgments

SunRISE GRL is sponsored by NASA grant #AWD006989, and hosted at the department of Climate and Space Sciences and Engineering (CLaSP), University of Michigan College of Engineering, Ann Arbor, MI. The authors are grateful for the GRL community whose participation and support makes this project possible.

7. Data Availability Statement

All data obtained for generating the plots in this manuscript are publicly available and can be retrieved on the project website: https://sunrise.umich.edu/. The catalog of identified SRB events observed by GRL is available online (Soni & Akhavan-Tafti, 2024). The data for CMEs and their associated flares, and Wind and are taken from http://cdaweb.gsfc.nasa.gov/istppub-lic/ and https://cdaw.gsfc.nasa.gov/CME_list/. The geomagnetic storms data is obtained from http://wdc.kugi.kyoto.u.ac.jp/dstrealtime/index.html.

This article is protected by copyright. All rights reserved.

Author Manuscript

8. References

Akhavan-Tafti, M. (2024). Training future space explorers. Science, 383(6688), 1188-1188.

Alibay, F., Kasper, J. C., Lazio, T. J. W., and Neilsen, T. (2017). “Sun radio interferometer space experiment (SunRISE): tracking particle acceleration and transport in the inner heliosphere,” in 2017 IEEE Aerospace Conference (Big Sky, MT), 1–15. doi: 10.1109/AERO.2017.7943789

Benz, A.O., 2009. 4.1. 1.6 Radio emission of the quiet Sun: 4 The Solar System; 4.1 The Sun; 4.1. 1 The quiet Sun. *Solar system*, pp.103-115.

Benz, A.O., 2009. 4.1. 2.8 Radio bursts of the non-thermal Sun: 4 The Solar System; 4.1 The Sun; 4.1. 2 Solar activity. *Solar System*, pp.189-203.

Bougeret, J.-L., M. L. Kaiser, P. J. Kellogg, R. Manning, K. Goetz, S. J. Monson, N. Monge, L. Friel, C. A. Meetre, C. Perche, L. Sitruk, and S. Hoang (1995), Waves: The Radio and Plasma Wave Investigation on the Wind Spacecraft, Space Sci. Rev., 71, 231–263, 10.1007/BF00751331.

Gopalswamy, N. and Torsti, J.: 2005, “Introduction to special section on Solar Coronal Mass Ejections and Energetic Particles”, Journal of Geophysical Research (Space Physics), 110, A12S00. doi:10.1029/2005JA011523.

Hettiarachchi, Y., Adassuriya, J., Jayaratne, C., Jayawardhana, S., & Monstein, C. (2024). The analysis of type II and type III solar radio bursts: GUI for the e-CALLISTO data. New Astronomy, 109, 102194.

Hicks, B. C., Paravastu-Dalal, N., Stewart, K. P., Erickson, W. C., Ray, P. S., Kassim, N. E., ... & Weiler, K. W. (2012). A wide-band, active antenna system for long wavelength radio astronomy. Publications of the Astronomical Society of the Pacific, 124(920), 1090.

Kasper, J., Lazio, J., Romero-Wolf, A., Lux, J., Neilsen, T., & SunRISE Science Team. (2020). The sun radio interferometer space experiment (sunrise) mission concept. In 2020 IEEE Aerospace Conference (pp. 1-12). IEEE.

Knock, S. A., and I. H. Cairns (2005), Type II radio emission predictions: Sources of coronal and interplanetary spectral structure, J. Geophys. Res., 110, A01101, doi:10.1029/2004JA010452.

Kumari, A., Morosan, D. E., Kilpua, E. K. J., and Daei, F., “Type II radio bursts and their association with coronal mass ejections in solar cycles 23 and 24”, Astronomy and Astrophysics, vol. 675, 2023. doi:10.1051/0004-6361/202244015.

Melrose, D. B. (2017). Coherent emission mechanisms in astrophysical plasmas. Reviews of Modern Plasma Physics, 1, 1-81.

This article is protected by copyright. All rights reserved.

Author Manuscript

Newkirk, G. Jr.: Astrophys. J. 133, 983 (1961). https://doi.org/10.1086/147104

Reid, H. A. S., (2020), “A Review of Recent Solar Type III Imaging Spectroscopy”, Front. Astron. Space Sci., Stellar and Solar Physics Vol. 7. doi.: 10.3389/fspas.2020.00056.

Reid, H. A. S., and Ratcliffe, H. (2014). A review of solar type III radio bursts. Res. Astron. Astrophys. 14, 773–804. doi: 10.1088/1674-4527/14/7/003.

Smerd, S. F., Sheridan, K. V., & Stewart, R. T. 1975, App. Lett., 16, 23.

Smerd, S. F., Sheridan, K. V., & Stewart, R. T. (1974, January). On split-band structure in type II radio bursts from the Sun. In Symposium-International Astronomical Union (Vol. 57, pp. 389-393). Cambridge University Press.

Soni, S. L., Akhavan-Tafti, M., Higgins, C., Fung, S., 2023, "SunRISE Ground Radio Lab: Engaging 2,500 Students and Educators in Hands-On, Heliophysics-focused, STEAM Activities", AGU23.

Suzuki, S., and Dulk, G. A. (1985). Bursts of Type III and Type V. Cambridge University Press.

Tsurutani, B. T., O. P. Verkhoglyadova, A. J. Mannucci, G. S. Lakhina, G. Li, and G. P. Zank (2009), A brief review of “solar flare effects” on the ionosphere, Radio Sci., 44, RS0A17, doi:10.1029/2008RS004029.

Cane, H. V., L. L. K. B., & S. R. (1986). Solar radio bursts. *Annual Review of Astronomy and Astrophysics*, 24, 211-248.

Ellingson, S. W., et al. (2009). The Long Wavelength Array. *IEEE Proceedings*, 97(4), 658-672.

Ellingson, S. W., et al. (2010). *The Long Wavelength Array: A Large HF/VHF Array for LWAMEMO*. Retrieved from LWA Memo.

Ellingson, S. W., et al. (2012). A wide-band, active antenna system for long wavelength radio astronomy. *IEEE Transactions on Antennas and Propagation*, 60(2), 782-790. DOI: 10.1109/TAP.2011.2171232.

Gopalswamy, N. Coronal Mass Ejections and Solar Radio Emissions. Retrieved from NASA Publications.

Gopalswamy, N.: In: Rucker, H.O., Kurth, W.S., Louarn, P., Fischer, G. (eds.) Coronal Mass Ejections and Solar Radio Emissions, Planetary, Solar and Heliospheric Radio Emissions (PRE VII), p. 325. Austrian Acad. Sci. Press, Vienna (2011)

Hick, P. P., et al. (2018). Real-time solar radio burst detection using machine learning. *Astronomy & Computing*, 25, 103-115.

This article is protected by copyright. All rights reserved.

Author Manuscript

Kassim, N. E., et al. (2007). The Long Wavelength Array: An Overview. *Proceedings of the IEEE*, 97(4), 646-653. DOI: 10.1109/JPROC.2008.916801.

Liu, S., et al. (2020). Solar radio bursts in the frequency range of 10–80 MHz. *Astrophysical Journal*, 891(1), 1-14.

Newkirk, G.A.: Annu. Rev. Astron. Astrophys. 5, 213 (1967).

Soni, S., Akhavan-Tafti, M., Higgins, C., and Fung, S. F., "SunRISE Ground Radio Lab: Engaging 2,500 Students and Educators in Hands-On, Heliophysics-focused, STEAM Activities", vol. 2023, Art. no. ED34A-06, 2023.

Soni, S.L., Ebenezer, E. & lal Yadav, M. Multi-wavelength analysis of CME-driven shock and Type II solar radio burst band-splitting. *Astrophys Space Sci* 366, 31 (2021). https://doi.org/10.1007/s10509-021-03933-7

Vemareddy, P. (2021). Eruption of the EUV Hot Channel from the Solar Limb and Associated Moving Type IV Radio Burst. Retrieved from IOPscience.

White, S. M., et al. (2011). Solar Radio Bursts: Observations and Theories. *Space Science Reviews*, 158(1-4), 1-19.

Vršnak, B., Aurass, H., Magdalenić, J., & Gopalswamy, N. (2001). Band-splitting of coronal and interplanetary type II bursts-I. Basic properties. Astronomy & Astrophysics, 377(1), 321-329.

Vasanth, V., & Umapathy, S. (2014). Studies on Longer Wavelength Type II Radio Bursts Associated with Flares and CMEs during the Rise and Decay Phase of 23rd Solar Cycle. Journal of Astrophysics, 2014(1), 168718.

Cunha-Silva, R. D., Fernandes, F. C. R., & Selhorst, C. L. (2015). Shock wave driven by CME evidenced by metric type II burst and EUV wave. Advances in Space Research, 56(12), 2804-2810.

Minta, F. N., Nozawa, S. I., Kozarev, K., Elsaid, A., & Mahrous, A. (2023). Solar radio bursts observations by Egypt-Alexandria CALLISTO spectrometer: First results. Advances in Space Research, 72(3), 844-853.

Cho, K. S., Lee, J., Gary, D. E., Moon, Y. J., & Park, Y. D. (2007). Magnetic field strength in the solar corona from type II band splitting. The Astrophysical Journal, 665(1), 799.

Gopalswamy, N. (2011). Coronal mass ejections and their heliospheric consequences. In First Asia-Pacific Solar Physics Meeting ASI Conference Series, 2011, Vol. 2, pp 241-258 Edited by Arnab Rai Choudhuri & Dipankar Banerjee (Vol. 2).

Author Manuscript

This article is protected by copyright. All rights reserved.

Kim, R. S., Gopalswamy, N., Moon, Y. J., Cho, K. S., & Yashiro, S. (2012). Magnetic field strength in the upper solar corona using white-light shock structures surrounding coronal mass ejections. The Astrophysical Journal, 746(2), 118.

Mann, G., Vocks, C., Warmuth, A., Magdalenic, J., Bisi, M., Carley, E., ... & Zucca, P. (2022). Excitation of Langmuir waves at shocks and solar type II radio bursts. Astronomy & Astrophysics, 660, A71.

Su, W., Li, T. M., Cheng, X., Feng, L., Zhang, P. J., Chen, P. F., ... & Zhang, L. Y. (2022). Quantifying the magnetic structure of a coronal shock producing a type II radio burst. The Astrophysical Journal, 929(2), 175.

Vršnak, B., Magdalenić, J., Aurass, H., & Mann, G. (2002). Band-splitting of coronal and interplanetary type II bursts-II. Coronal magnetic field and Alfvén velocity. Astronomy & astrophysics, 396(2), 673-682.

Ramesh, R., Kathiravan, C., & Sastry, C. V. (2010). Estimation of magnetic field in the solar coronal streamers through low frequency radio observations. The Astrophysical Journal, 711(2), 1029.

Soni, S. L., & Akhavan-Tafti, M. (2024). Catalog for Solar Radio Bursts Observed by SunRISE Ground Radio Lab (GRL): Jan-July 2024 [Dataset]. University of Michigan - Deep Blue Data. https://doi.org/10.7302/E4BH-MJ50

Gopalswamy, N., Yashiro, S., Michalek, G., Xie, H., Lepping, R. P., & Howard, R. A. (2005). Solar source of the largest geomagnetic storm of cycle 23. Geophysical research letters, 32(12).

Melrose, D. B. (2017). Current-driven flare and CME models. Journal of Geophysical Research: Space Physics, 122(8), 7963-7978.

Nelson, S. P. (2014). Design, fabrication, and testing of a data acquisition and control system for an internally-calibrated wide-band microwave airborne radiometer (Master's thesis, Colorado State University).

Vasanth, V., Umapathy, S., Vršnak, B., Žic, T., & Prakash, O. (2014). Investigation of the coronal magnetic field using a type II solar radio burst. Solar physics, 289, 251-261.

Higgins, C. A., Thieman, J. R., Nakamura, B., & Dorcey, R. (2010, December). GAVRT and Radio Jove: Partners in K-12 Science Teacher Training. In AGU Fall Meeting Abstracts (Vol. 2010, pp. ED53A-0527).

Newkirk Jr, G. (1967). Structure of the solar corona. Annual Review of Astronomy and Astrophysics, vol. 5, p. 213, 5, 213.

This article is protected by copyright. All rights reserved.

Author Manuscript

Soni, S. L., & Ebenezer, E. (2022). Kinematics and interplanetary characteristics of a halo Coronal Mass Ejection: a multi-wavelength analysis. Astrophysics and Space Science, 367(4), 40.

Author Manuscript

This article is protected by copyright. All rights reserved.

Author Manuscript

Appendix A: SunRISE Ground Radio Lab Logistics

A. SunRISE GRL Radio Kit

The SunRISE dual dipole antenna (DDA) kit, also referred to as the SunRISE GRL antenna kit, is based on a simple dual dipole antenna configuration. The radio receiver hardware and software were supplied by NASA's Radio JOVE project. The antenna hardware was redesigned by a team of undergraduate and graduate students at the University of Michigan with the goal of making them easy to install by high school students nationwide (Akhavan-Tafti, 2024).

Radio JOVE (https://radiojove.gsfc.nasa.gov/) (Higgins et al., 2010) started as a NASA-sponsored project in 1999 and developed a hands-on radio telescope kit suitable for education and outreach. Currently, Radio JOVE is a NASA partner citizen science project using a multi-frequency radio telescope that is built and operated by participants to make scientific observations of Jupiter, the Sun, the Milky Way Galaxy, and Earth-based radio emissions. Participants may build a simple radio telescope kit, make scientific observations, and interact with near-professional radio observatories in real-time over the Internet.

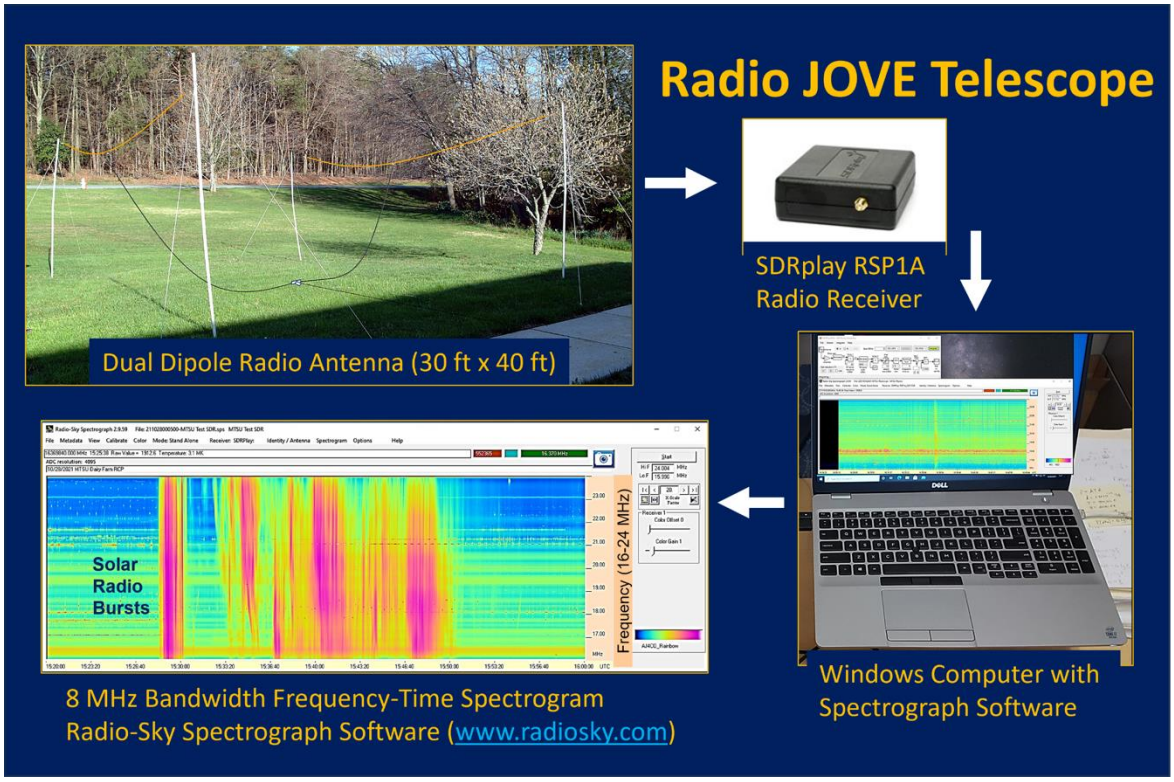


Figure A.1. The Radio JOVE spectrograph radio telescope kit. The panels show the dual dipole antenna, the SDRplay RSP1A model radio receiver, and a computer with the Radio-Sky Spectrograph software. The example spectrograph shows many solar radio bursts (red vertical bands) from 16 to 24 MHz. Horizontal bands are distant and local stations and interference. Image courtesy of Radio JOVE.

This article is protected by copyright. All rights reserved.

Radio JOVE uses standard hardware for an affordable, kit-based radio spectrograph including a dual-dipole antenna and a commercial wideband software-defined radio (SDR), as shown in Figure A.1. The Radio-Sky Spectrograph (RSS) software (www.radiosky.com) and its associated SDRPlay2RSS program were developed for Radio JOVE to provide control of the radio as well as data display, recording, and analysis. The spectrograph system can address science questions related to heliophysics, planetary and space weather science, and radio wave propagation.

B. Self-Paced, Training Modules

The SunRISE GRL project further aims to educate high school students on topics including radio astronomy and space weather. The initial stage in developing the self-paced training modules was to define specific learning objectives. We aimed to provide participants with a comprehensive understanding of the concepts of solar radio astronomy, radio antenna set-up, data analysis techniques, and applications in space weather monitoring. These goals served as the foundation for content creation. Understanding the target demographic was essential for tailoring the modules effectively. All students and educators worldwide have access to the modules through the Canvas platform, and all training videos are uploaded on the SunRISE Ground Radio Lab's Youtube channel, @SunRISE_GRL.

i. Structure of Modules

The modules are divided into multiple sections to ensure a consistent and logical flow of content. Each module begins with a brief overview of the topic along with specific learning objectives. Next, the audience is presented with the lesson, selected from topics ranging from solar physics, radio astronomy, radio basics and operation instructions, data acquisition and processing instructions, as well as a brief guide to citizen science opportunities, as summarized in Table A.1. To enhance learning and emphasize real-world applicability, each lesson includes practical applications, resources, and case studies.

ii. Engaging Multimedia Elements

To enhance the learning experience, engaging multimedia elements are incorporated into the modules, including high-resolution images, interactive visualizations, audio and video clips to illustrate solar astronomy, radio phenomena, instrument setups, and data analysis processes. These multimedia elements brought the subject matter to life and facilitated a deeper understanding of complex concepts.

iii. Interactive Activities and Assessments

Various interactive activities are integrated to encourage active learning and self-assessment. These activities included data analysis exercises, hands-on simulations, and lesson quizzes, as shown in Figure A.2, to reinforce comprehension and gauge progress. The step-by-step activities and self-assessment progressively guide the audience in applying the acquired knowledge to interpret solar radio data and solve relevant space science-focused challenges.

This article is protected by copyright. All rights reserved.

Author Manuscript

Author Manuscript

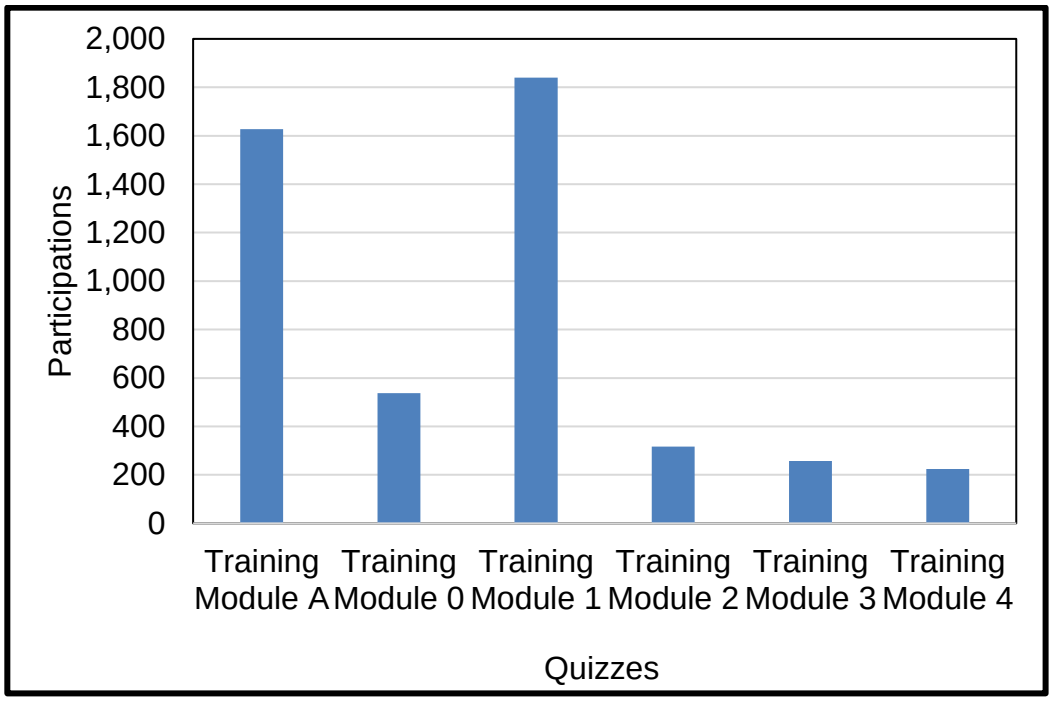


Figure A.2: Every training module set is concluded with a quiz, intended to test participants' understanding of the material before they are allowed to proceed to the following module. participants who complete all Training Modules successfully will be issued a signed copy of a NASA Certificate of Completion.

iv. Clear and Accessible Language

To ensure accessibility, clear and concise language are presented throughout the modules. Technical terms and complex concepts are explained in a user-friendly manner, allowing the audience to grasp the material regardless of their previous knowledge in the field. Definitions, explanations, and examples were provided to facilitate comprehension and enhance the learning experience. Text, image, and audio are used to present the materials to ensure reaching a broad audience and learning skills and preferences. Additional resources further facilitated self-paced learning beyond the core content of the modules, including research papers, relevant publications, and online databases that allowed participants to delve deeper into specific topics or pursue advanced studies in solar radio astronomy.

Table A.1: Syllabus for the self-paced training modules.

#	**Section**	**Sub-section**
1	Introduction: SunRISE Mission / SunRISE GRL/ Radio JOVE	-
2	Introduction: The Sun	2.1 Solar interior

This article is protected by copyright. All rights reserved.

		2.2 Solar atmosphere 2.3 Solar Activity 2.4 Space weather
3	Radio Science Background	3.1 Intro to Radio Astronomy 3.2 Radio wave propagation 3.3 Solar radio emissions 3.4 Jupiter radio emissions 3.5 Galactic radio emissions
4	Radio Telescope Operation	4.1 Dual Dipole Setup and operation 4.2 Data collection (making the data scientific, metadata, timing, etc.) 4.3 Antenna phasing 4.4 Archiving your data
5	Solar Radio Burst Analysis: Exploring the Mysteries of the Sun	5.1 Solar Radio burst Identifications 5.2 Investigating the Relationship between Solar Radio Bursts and Space Weather 5.3 Future Directions and Collaborative Efforts
6	Citizen Science	6.1 Overview of CitSci projects 6.2 Guide to contribute and participate 6.3 Presentations and Publications

C. The SunRISE GRL Team

The SunRISE GRL team is led by Mojtaba Akhavan-Tafti at the University of Michigan. Akhavan-Tafti leads a team of postdoctoral fellows, undergraduate and graduate students, as well as high school teachers and students. The team affiliations include University of Michigan (UM), Middle Tennessee State University (TMSU), Goddard Space Flight Center (GSFC), Dalton State College (DSC), Washtenaw Community College (WCC), Washtenaw Technical Middle College (WTMC).

D. Measuring Student Learning Outcomes

To effectively gauge student learning outcomes, a combination of assessment methods, feedback surveys, and engagement tracking is employed throughout the program. To measure the students' knowledge and understanding of key space science concepts and radio telescope technologies, a quiz is provided at the end of each module. The required quizzes cover topics such as radio astronomy, space physics, and radio astronomy instrumentation, aligning with the curriculum delivered during the project.

A shown in Figure A.3, student engagement is tracked by monitoring participation in different project components, such as: attendance in workshops, webinars, and hands-on activities, involvement in discussions and group projects, as well as contributions to project outcomes, such as data analysis or radio telescope installations. Tracking

This article is protected by copyright. All rights reserved.

Author Manuscript

engagement helps to identify students who are highly engaged and those who may need additional support, allowing for personalized intervention, if necessary.

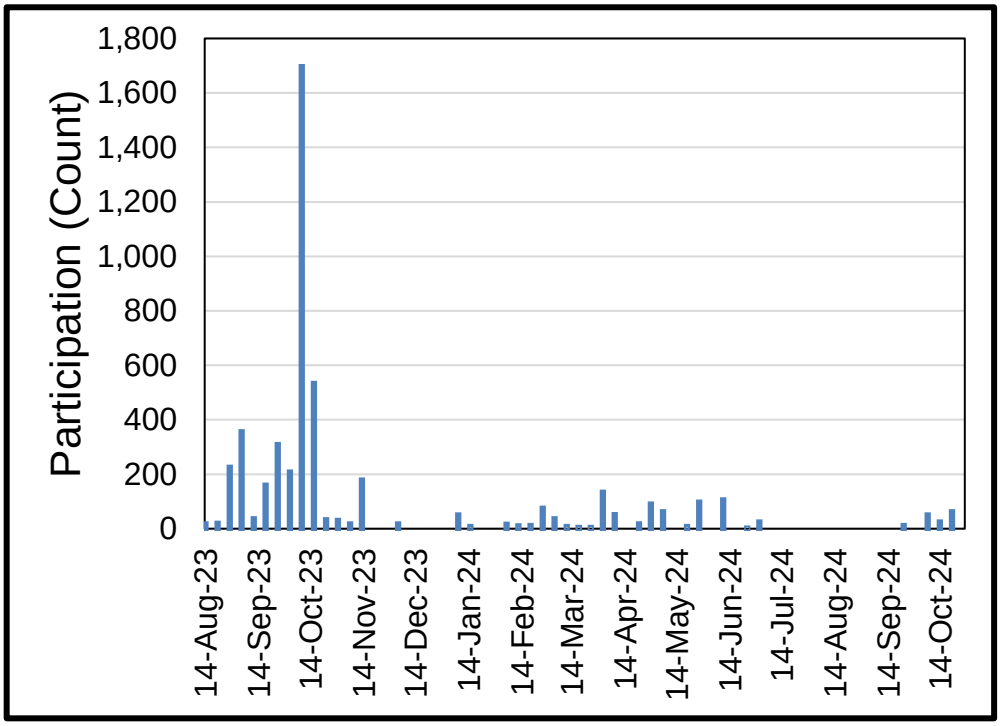


Figure A.3 shows the average weekly student participation since the inception of the program in late Summer 2023. As the figure shows, up to 1,700 activities were recorded on our online platform per week.

At various stages of the program, students are asked to complete anonymous feedback surveys. These surveys focus on topics including students' perceived understanding of the subject matter before and after participating in the program, interest levels in space science and technology fields, satisfaction with the structure and content of the program, as well as feedback on hands-on experiences such as working with radio telescope data or building antennas. This qualitative data provides insights into how well the program meets students' needs and sparks interest in STEAM fields. It also allows us to identify areas for improvement in future iterations.

E. Trainings in Operating Antennas and Analyzing Data

ii. Training in Operating the GRL Antennas

Students receive extensive training in the operation of GRL antenna through self-training modules. This training module set covers: 1) Antenna setup: students are taught how to physically install the antenna, ensuring proper orientation and calibration. They learn about the importance of minimizing noise interference and environmental factors, such as weather, that can impact data collection, 2) Understanding Signal Reception: training includes explaining how antennas receive radio signals from Sun, and how these signals are processed. This theoretical foundation helps students appreciate the importance of

This article is protected by copyright. All rights reserved.

Author Manuscript

correct antenna configuration for clear data reception, and 3) Use of Software Tools: students are introduced to specialized software for monitoring antenna performance and managing data collection. They learn how to adjust operational parameters and remotely control the antennas during observational sessions.

iii. Training in Data Analysis

Once data is collected, participants upload their data to the GRL data repository. Participants can access all archived data across all GRL stations nationwide to compare with their own observations. The SunRISE GRL team at University of Michigan provides various data analysis techniques to the participants, such as visualization and interpretation, signal processing etc. Through this, students learn to use visualization software to graphically represent the data and interpret results. They also learn about signal processing, including cleaning and processing raw data, noise removal, and more.

iv. Overcoming Challenges in Real-World Data Collection

Real-world data collection often presents several challenges that students must navigate. For instance, environmental interference, such as weather conditions (rain, lightning, or high winds) can impact antenna performance, causing signal distortion. Students are trained to monitor and account for such conditions during data collection. Earth-based human activities, such as local radio transmissions, can introduce unwanted noise into the data. Students may further encounter issues with antenna malfunctions, such as hardware malfunctions, misaligned antennas, or connectivity problems. These technical difficulties can lead to incomplete or corrupted data. Students learn to identify and filter out this interference using data cleaning algorithms.

v. Support in Troubleshooting Issues and Ongoing Expert Guidance

To help participants handle challenges, the program provides structured guidance. Students are given protocols to follow when problems arise. For example, they learn how to systematically check antenna connections, recalibrate settings, or run diagnostic tests on the equipment. Regular monthly workshops are conducted where students can discuss their issues directly with project leads. Students are supported by mentor space scientists and engineers, who provide ongoing guidance throughout the project. While expert guidance is readily available, the goal of the program is to equip students with the skills to handle technical challenges independently.

vi. Impact on STEAM Interests: Survey Results

Participation in the SunRISE GRL project has had a positive influence on students' interest in STEAM fields, as evidenced by both quantitative and qualitative data:

- Data from post-program surveys show a significant increase in the number of students expressing an interest in pursuing careers in STEAM. For example, in a recent cohort, over 75% of students reported a heightened interest in space science or engineering after completing the program.

This article is protected by copyright. All rights reserved.

Author Manuscript

- Several students have provided feedback on how the program inspired them to explore careers in space technology, engineering, or related fields. Mentorship by professional engineers and scientists, along with the hands-on aspect of working with cutting-edge technology, have been particularly impactful.

F. Participating High Schools

To date, more than a dozen high schools have received free antenna kits and access to our online platform. The participating high schools include:

1. Belmont High School, Belmont, MA
2. CROEM High School, Boqueron, PR
3. Sault Area High School, Sault Ste. Marie, MI
4. Coral Reef High School, Miami, FL
5. Skyline High School, Ann Arbor, MI
6. Trinity Christian School, Morgantown, WV
7. Hamtramck High School, Hamtramck, MI
8. Morrison High School, Morrison,IL
9. Centennial High School, Circle Pines, MN
10. Ann Arbor Huron High School, Ann Arbor, MI
11. Central Magnet School, Murfreesboro, TN
12. Marquette Senior High School, Marquette, MI
13. Saline High School, Saline, MI
14. Tahquamenon Area Schools, Newberry, MI
15. BioTECH @ Richmond Heights 9-12, Miami, FL
16. Vel Phillips Memorial High School, Madison, WI
17. Franklin High School, Franklin, NH
18. Washtenaw Technical Middle College, Ann Arbor, MI

The SunRISE GRL's free of charge hardware and online platform have removed many barriers to participation. The high schools are distributed throughout the United States, with different demographics: some high schools are located in rural areas, while others are in densely populated areas, some high schools created extra-curricular activities around SunRISE GRL program for their students to participate in, while some high schools relied on students and parents to step in to help.

G. Summer Internship

In an effort to bridge the gap between our high school demographics, and to encourage further STEAM participation, the GRL team recruited 7 high school student volunteers to participate in a remote, summer-long internship to help us process and catalog SRB data and to analyze them. The students were nominated by teachers for their outstanding academic standing and contribution to SunRISE GRL activities. Over the course of Summer 2023, student worked alongside our team. The culmination of their efforts was a science poster presentation at the Solar Heliospheric and INterplanetary Environment (SHINE) workshop in Juneau, AK.

This article is protected by copyright. All rights reserved.

Author Manuscript

9. SunRISE GRL Archive: Format, Access, and Research Contributions

The SunRISE GRL catalog of SRBs is a comprehensive and publicly accessible database of the observed radio bursts at various GRL stations nationwide. The catalog is an ongoing effort maintained by students and mentors, providing valuable data to the scientific community in support of the broader objectives of the SunRISE mission.

a. Data Collection Process

The data collection process in the SunRISE GRL is designed to provide students with hands-on experience in operating ground-based radio telescopes, collecting solar radio burst data, and ensuring data accuracy through multiple validation techniques. The process involves several stages, from setting up the equipment to final data analysis and cataloging.

b. Equipment Setup and Calibration:

Participants begin by installing the GRL antennas at various stations. Before starting data collection, the antennas and receivers are calibrated to ensure accuracy. Calibration accounts for local environmental factors and signal interference, including ionospheric conditions. This step ensures that the data collected will reflect true solar radio emissions rather than noise or distortion.

c. Data Acquisition

Once calibrated, the receiver begins recording raw data. This stage involves real-time monitoring to detct solar radio bursts. GRL employs advanced techniques, such as multi-frequency observation and dual-station comparison, to filter out terrestrial interference and ionospheric effects. By observing at multiple frequencies, the user can distinguish genuine solar signals from distortions caused by the ionosphere.

d. Data Processing

The raw data undergoes initial filtering to remove local interference, such as signals from terrestrial radio stations, electronics, or environmental noise. GRL also addresses the issue of ionospheric interference, a common challenge in ground-based radio astronomy where the Earth's ionosphere can distort, delay, or weaken incoming radio signals, especially at lower frequencies. This interference can lead to inaccuracies in detecting SRBs and other celestial events. To counteract these effects and ensure reliable data collection, the GRL implements a variety of strategies. These include the use of multi-frequency observations to differentiate true solar signals from ionospheric distortions, leveraging dual-station comparisons across different geographic locations to identify and filter out localized ionospheric effects.

e. General Layout of the Catalog

Author Manuscript

This article is protected by copyright. All rights reserved.

The GRL SRB catalog is structured to systematically categorize SRBs based on their characteristics and possible origins, providing both a user-friendly interface and in-depth scientific information for researchers. The catalog includes the following components:

a. Basic Information: Each SRB entry includes key observational details such as the date and time of detection, type of SRB (e.g., Type II, Type III, etc.), frequency range, and location of the GRL station.

b. Associated Solar Events: When available, the catalog associates SRBs with concurrent solar phenomena, such as flares and Coronal Mass Ejections (CMEs). This contextual data helps researchers draw correlations between the radio bursts and solar events.

c. Indices and Cross-References: The catalog provides a matrix of indices (as shown in Table 3), linking SRBs to other observed solar phenomena. This matrix includes:

    1. Radio Burst Characteristics: Characteristics of the detected radio bursts, including their duration, intensity, and frequency spectrum.

    2. Solar Flares: Information about any associated flares, including flare classification (C, M, X classes), peak intensity, and duration.

    3. Coronal Mass Ejections (CMEs): Data on CMEs that may have coincided with SRBs, including their velocity, location, and propagation direction.

    4. Source Regions: Identification of active regions on the Sun that may have triggered SRBs and solar eruptions.

d. Supporting Documentation: Accompanying the catalog are several supportive resources, including:

    1. Complete Description of the Catalog: Detailed documentation explaining how to interpret the data and navigate the catalog.

    2. Related Links: Hyperlinks to external resources on SRBs, solar flares, and CMEs, along with tools to help visualize solar phenomena.

Researchers can access a text-only version of the SRB catalog that lists the basic observational details of the SRBs. This version omits plots and detailed tables of measured parameters and serves as a convenient reference for basic information.

f. Access to the Catalog:

The SunRISE GRL SRB catalog is publicly accessible via the following DOI link:. https://doi.org/10.7302/e4bh-mj50 The catalog is hosted on a secure platform, providing easy access to both the scientific community and interested citizen scientists. Users can:

Author Manuscript

This article is protected by copyright. All rights reserved.

a. Search the catalog by date, SRB type, or associated solar events to locate relevant data.

b. Download the data for use in their own research projects, with options to export data in formats compatible with analysis software (e.g., CSV, JSON).

g. Using the data for Research

The structured format of the GRL SRB catalog allows researchers to perform a wide variety of analyses. For example, scientists can:

a. Identify Patterns in SRBs: By comparing SRBs recorded at different stations and during different solar conditions, researchers can identify recurring patterns or anomalies in the data, contributing to a better understanding of the underlying physics of these bursts.

b. Correlate SRBs with Solar Activity: The inclusion of flare and CME data enables researchers to investigate correlations between solar eruptions and radio bursts, leading to new insights into the triggers and propagation mechanisms of SRBs.

c. Compare SRB Data Across Time and Location: The multi-station nature of the GRL project allows for comparisons of SRBs recorded at different geographical locations, helping scientists examine the spatial variation in solar radio emissions and their interaction with Earth's atmosphere.

d. Collaborative Research: The catalog provides data that could be integrated into larger datasets from other solar missions, allowing for collaborative multi-mission studies on solar activity and space weather.

Table A.2 provides a sample dataset from the GRL SRB catalog. It is a matrix of indices such as Radio Burst, Flare, CMEs, and sources. A set of supportive documents are provided with the catalog (i) a complete description of the Catalog, (ii) related links useful for SRB and associated solar phenomena. The text-only version lists all the basic information about the SRBs, except for plots, and tables of measured parameters of associated solar events. The SunRISE GRL catalog is available at https://doi.org/10.7302/e4bh-mj50

Table A.2: Formatting of the SunRISE GRL SRB catalog.

#	**Solar Radio Bursts**				**Flares**				**CME**			**GRL Stations**
	Date	Start (UT)	End (UT)	Type	Start (UT)	Peak (UT)	End (UT)	Class	Date	Time	Velocity	
1	2-2-24	16:30	16:34	III	16:30	16:32	16:34	C3.1	2-2-24	NA	NA	Skyline, Ann Arbor, MI

This article is protected by copyright. All rights reserved.

												Peach Mountain, Dexter, MI
2	2-12-24	19:26	19:29	III	19:26	19:27	19:29	C7	2-12-24	NA	NA	Skyline, Ann Arbor, MI Peach Mountain, Dexter, MI
3	3-23-24	17:12	17:13	III	16:40	16:50	17:17	M5	3-23-24	NA	NA	Skyline, Ann Arbor, MI Peach Mountain, Dexter, MI

10. Future Direction

The SunRISE GRL project is the outreach and communications component of the NASA SunRISE mission. The mission team is committed to continuing to support the outreach project throughout the life of the mission. This includes continuing to provide antenna kits free of charge to interested high schools in the United States. Our online platform is and will remain available to all students worldwide, free of charge. All training materials are also available on YouTube.

H. Monthly Webinars

The SunRISE GRL monthly webinar series commenced in September 2023, with the goal of 1) maintaining student engagement through recurring activities, including learning about the SunRISE mission and its objectives from the SunRISE leadership team and other space science and radio astronomy experts, as well as 2) providing a platform for the students to ask questions and participate in ongoing data collection and analysis. The webinars helped to successfully encourage students to install their antenna kits and collect data during the solar eclipses of 2023 and 2024. To date, fourteen webinars have been held with keynote speakers ranging from the SunRISE leadership team, including Dr. Justin Kasper, the PI of the SunRISE mission, to radio astronomy and space systems engineering experts. Figure A.4 summarizes the number of participants during each monthly webinar. In some instances, our high school teachers join our webinars and broadcast the webinar live to their class.

Author Manuscript

This article is protected by copyright. All rights reserved.

Author Manuscript

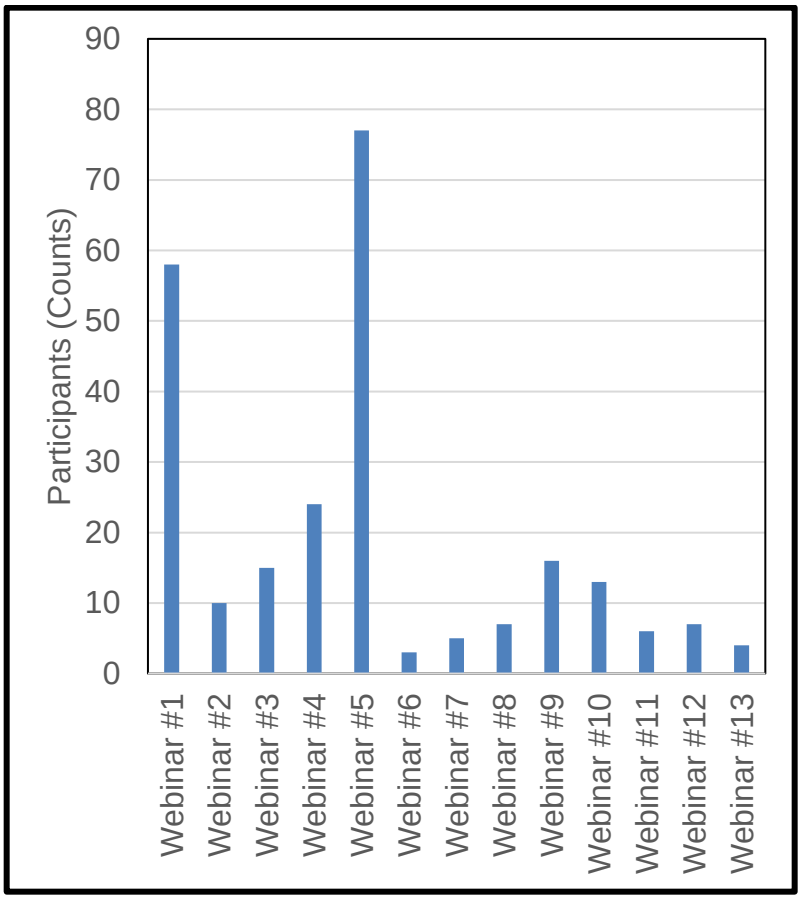


Figure A.4: Webinar participation in years 2023 and 2024. One participant does not correspond to one student. In some cases, one participant refers to a classroom full of high school student wherein the teacher registers and joins the webinar and broadcast it live to his or her students.

11. Interested High Schools

Interested high schools in the United States and territories are encouraged to discuss the project with their administration and submit a request form to receive a free SunRISE GRL antenna kit, as well as access to our self-paced, online training modules. For more information, and to submit a query, please visit: https://sunrise.umich.edu/.

This article is protected by copyright. All rights reserved.